Synthesis of Biotinylated α-D-Mannoside or *N*-Acetyl *β*-D-Glucosaminoside Decorated Gold Nanoparticles: Study of Their Biomolecular Recognition with Con A and WGA Lectins

Xiaoze Jiang,[†,‡] Abdelghani Housni,[†,‡] Guillaume Gody,[§,||] Paul Boullanger,[||] Marie-Thérèse Charreyre,*[,§,⊥] Thierry Delair,[§] and Ravin Narain*[,†,‡]

Department of Chemical and Materials Engineering, University of Alberta, ECERF, Edmonton, Alberta T6G2G6, Canada, Department of Chemistry and Biochemistry, Laurentian University, 935, Ramsey Lake Road, P3E 2C6, ON, Canada, Unité Mixte CNRS-bioMérieux, Ecole Normale Supérieure de Lyon, IFR 128, 46 allée d'Italie, 69364 Lyon Cedex 07, France, and Laboratoire de Chimie Organique II, UMR 5622 CNRS/UCBL, 69616 Villeurbanne Cedex, France. Received September 30, 2009; Revised Manuscript Received January 6, 2010

Gold nanoparticles (NPs) functionalized with a mixed shell of well-defined biotinylated glycopolymers and polyethylene glycol (PEG) provide an effective platform for the biomolecular recognition of proteins both in solution and on surfaces. Well-defined biotinylated glycopolymers were first synthesized by the reversible addition−fragmentation chain transfer (RAFT) process. They contain two types of carbohydrate residues either *N*-acetyl *β*-D-glucosaminopyranoside (**GlcNAc**) or α-D-mannopyranoside (**Man**) as pendent groups. The biotinylated glycopolymers and polyethylene glycol were subsequently used in the *in situ* formation of gold glyconanoparticles via an easy photochemical process. The obtained biotinylated glyconanoparticles were characterized by dynamic light scattering (DLS) and transmission electron microscopy (TEM). The bioavailability of the biotin and specific carbohydrate residues at the periphery of the NPs were assessed using the diffraction optic technology (DOT) system. The studies showed the accessibility of the biotin ligands for conjugation to immobilized avidin on the DOTLab biosensor. Furthermore, these avidin conjugated glyconanoparticles were found to selectively immobilize lectins. The specificity of lectin binding was dependent on the type of carbohydrate residues. As such, *N*-acetyl *β*-D-glucosaminoside decorated gold nanoparticles were found to specifically interact with wheat germ agglutinin (WGA) lectin, whereas α-D-mannoside ones were found to specifically interact with Concanavalin A (Con A) lectin.

INTRODUCTION

Gold nanoparticles are receiving enormous attention as they are very promising for biomolecular applications such as labeling, detection, and transfer of genetic materials (*1*).To improve the water stability of synthesized gold cores, different methods were used to prepare water-dispersible and size-tunable gold nanoparticles via the reduction of gold salts in the presence of appropriate stabilizing agents that prevent particle aggregation (*2–6*). Among the preparation methods of gold nanoparticles, the gold salts, chloroaurate ($AuCl_4^-$), were usually reduced with a reducing agent such as sodium tetrahydroborate ($NaBH_4$) in the presence of the desired capping ligands.

Recently, a new photochemical method, reported by Scaiano et al. (*7*), was used to prepare unprotected water-soluble gold nanoparticles via the reduction of $HAuCl_4$ by photochemical decomposition of Irgacure-2959, a water-soluble benzoin, under mild conditions in one step. The preparation process of gold nanoparticles is fast from seconds to minutes, and their sizes could be easily controlled by the intensity of illumination (UV). Following this principle, ligand functionalized water-soluble gold nanoparticles such as biotinylated glyconanoparticles (*8*) and BSA protein-stabilized gold nanoparticles (*9*) have been prepared by our groups via a photochemical process. This method would be a versatile approach for the preparation of surface-coated gold nanoparticles with RAFT prepared polymers.

Focusing on their actual applications in biomedicine and biotechnology, we believe that it is important to consider the surface chemistry for the long-term stability of gold nanoparticles and their biocompatibility. It has been reported that a variety of biocompatible molecules such as proteins (*10, 11*), polyethylene glycol (PEG) (*12*), DNA (*13, 14*), and carbohydrate moieties (*8, 15*) have been utilized to stabilize gold nanoparticles. Following the development of living radical polymerization, various water-soluble polymers with versatile composition and functionality prepared by RAFT polymerization (*16*) were exploited to modify the surface of gold nanoparticles as stabilizers via thiol chemistry after the reduction of the thiocarbonylthio chain-end.

The incorporation of these water-soluble polymers into the shell of gold nanoparticles not only provides a protective shield to prevent their aggregation but also introduces new functions at their periphery. Another important aspect of the surface immobilized polymers bearing reactive functional groups is to provide an opportunity for further surface functionalization. It has been shown that the polymers can tailor the properties of nanoparticles and that the gold cores can also modify the physical properties of polymers (*17–21*).

* To whom correspondence should be addressed. (M.-T.C.) Phone: (+33) (0)4 72728938. Fax: (+33) (0)4 72728787. E-mail: marie-therese.charreyre@ens-lyon.fr. (R.N.) Phone: (780) 492-1736or (705) 675-1151ext. 2186. Fax: (780) 492 1736 or (705) 675-4844. E-mail: narain@ualberta.ca or rnarain@laurentian.ca.

† University of Alberta.

‡ Laurentian University.

§ Unité Mixte CNRS-bioMérieux.

|| UMR 5622 CNRS/UCBL.

⊥ Current address: Laboratoire Joliot-Curie et Laboratoire Ingenierie des Materiaux Polymeres, Ecole Normale Supérieure de Lyon, IFR128, 46 Allee d'Italie 69364 Lyon Cedex 07, France.

10.1021/bc900431p
Published on Web 02/03/2010

Carbohydrate modified gold nanoparticles have recently attracted much attention since lectin−carbohydrate interactions play crucial roles in a variety of biological processes, including fertilization, cell migration, cancer, and host−pathogen interactions (*22, 23*). Using the gold nanoparticles as a carrier, the outer carbohydrate moieties located on the surface as many antennae increase the ability of carbohydrate−protein interaction as a result of the cluster glycoside effect (*24, 25*). Russell et al. reported the study of gold nanoparticles stabilized with a self-assembled monolayer of a mannose derivative, 2-mercaptoethyl α-D-mannopyranoside, and exploited the α-D-mannoside decorated nanoparticles to examine the binding specificity of the well-known lectin, Concanavalin A (Con A), using UV−visible spectrophotometry (*15*). Lactose-conjugated gold nanoparticles reported by Kataoka et al. (*26*) were prepared from PEG-stabilized gold nanoparticles bearing acetal groups on the outer shell, by reaction with *p*-aminophenyl-*a*-lactosyl. These *a*-lactosyl decorated nanoparticles exhibit specific recognition of *Recinus communis* agglutinin (RCA_{120}) and could be applied in bioassays and biorecognition. Although these nanoparticles were successfully used to study the carbohydrate−lectin interactions, this study was limited to only one kind of lectins and one type of carbohydrate.

In order to investigate the lectin−carbohydrate interaction mechanism, many systems bearing different carbohydrate (or lectin) moieties were developed to study the specific interaction with different lectins (or carbohydrates) by different approaches such as the surface plasmon resonance (SPR), quartz crystal microbalance (QCM), isothermal titration calorimetry (ITC), fluorescence techniques, atomic force microscopy (AFM), and electrochemical impedance spectroscopy (EIS) (*25, 27–32*). Although existing approaches have been partially successful, these reported methods usually require extensive instrumental setup and synthetic complication for the fixation of the targeted group (carbohydrate or lectin) onto the surface of the sensor, which obviously limited the investigation of their interactions. Accordingly, a sensitive, rapid, simple, reliable, and cost-effective method should be found to study these interactions.

Herein, we describe the synthesis of well-defined biotinylated glycopolymers via the RAFT polymerization process. The obtained glycopolymers containing two types of carbohydrate residues, either *N*-acetyl β-D-glucosaminoside (**GlcNAc**) or α-D-mannoside (**Man**) as pendent groups, were subsequently used with PEG for the *in situ* formation of glyconanoparticles via a photochemical process. Combining the photochemical method and RAFT process, different surface-functionalized gold nanoparticles were prepared with or without the biotin and/or the carbohydrate moieties. The obtained nanoparticles were characterized by dynamic light scattering (DLS) and transmission electron microscopy (TEM). To access the availability of the biotin and specific carbohydrate residues located on the nanoparticle surface, a simple instrument, diffraction optics technology (DOT) system, was used to probe the attachment of biotinylated nanoparticles on the surface of the avidin sensor chip, which further provided the possibility of studying specific lectin−carbohydrate interactions between the carbohydrates (GlcNAc or Man) and the lectins (WGA or Con A).

EXPERIMENTAL SECTION

Materials. *N*-Acryloylmorpholine (NAM) (Aldrich, 97%) was distilled under reduced pressure (120 °C, 10 mmHg). 2,2′-Azobis(isobutyronitrile) (AIBN) (Fluka, 98%) was purified by recrystallization from ethanol. 1,4-Dioxane (Acros, 99%) was distilled over $LiAlH_4$ (110 °C). Trioxane (Acros, 99%), EZ-Link Biotin PEO-Amine ((+)-biotinyl-3, 6-dioxaoctanediamine, Pierce), and other materials were used without further purification. Syntheses of *tert*-butyl dithiobenzoate (*t*BDB) (*21*) and *N*-[8-((+)-biotinamido)-3,6-dixoaoctyl]-2-[[2-phenyl-1-thioxoethyl]thio]-propanamide (BEDBA) (*33*) have been described previously. Syntheses of the mannose derivative, 8-acrylamido-3,6-dioxaoctyl 2,3,4,6-tetra-*O*-acetyl-α-D-mannopyranoside (ManAm), and of the *N*-acetyl-glucosamine derivative, 8-acrylamido-3,6-dioxaoctyl 2-acetamido-3,4,6-tri-*O*-acetyl-2-deoxy-β-D-glucopyranoside (GlcNAcAm), have been described elsewhere (*34*). Synthesis of the biotinylated PNAM homopolymers has been described previously (*33*). Biotin-CTA, *N*-[8-((+)-biotinamido)-3,6-dioxaoctyl]-2-[[2-phenyl-1-thioxo]thio]-4-cyanopentanoate (BCBDBA), was synthesized from succinimido-4-[[2-phenyl-1-thioxo]thio]-4-cyanopentanoate and (+)-biotinyl-3,6-dioxaoctanediamine as shown in Figure S1 in Supporting Information. The photoinitiator, Irgacure-2959, was given by CIBA Specialty Chemicals.

RAFT Polymerization of the Mannose and *N*-Acetylglucosamine Derivatives (ManAm and GlcNAcAm) with Biotin-CTA. RAFT copolymerization of ManAm or GlcNAcAm with *N*-acryloylmorpholine in the presence of biotin-CTA (BCBDBA) has been performed (shown in Schemes 1 and 2) using a procedure similar to that recently reported for a Galactose derivative (*35*) except that the reaction was performed directly inside the NMR spectrometer.

Typical runs for ManAm and for GlcNAcAm are described below. NAM (91 mg, 0.65 mmol), ManAm (85 mg, 0.16 mmol), biotin-CTA (BCBDBA, 7.3 mg, 0.011 mmol), AIBN (0.31 mg, 1.9×10^{-3} mmol), 1,4-d_8-dioxane (423 μL), and trioxane (2.3 mg, internal reference for ^{1}H NMR determination of monomer consumption) (*36*) were introduced in a NMR tube fitted with a Young's valve. The mixture was degassed by five freeze−evacuate−thaw cycles. A first NMR acquisition was carried out at 27 °C. Then, the tube was removed, and the temperature was set at 75 °C. The tube was then reintroduced (time t_0), and acquisitions were regularly performed. The progress of the reaction was monitored by the disappearance of the vinyl proton signals, by comparison of the vinyl protons of NAM (5.7 ppm) and of ManAm (5.6 ppm) with trioxane (5.08 ppm).

NAM (108 mg, 0.765 mmol), GlcNAcAm (102 mg, 0.192 mmol), biotin-CTA (BCBDBA, 1.74 mg, 2.74×10^{-3} mmol), AIBN (0.045 mg, 2.74×10^{-4} mmol), and 1,4-d_8-dioxane (504 μL) were introduced in a NMR tube fitted with a Young's valve. The mixture was degassed by five freeze−evacuate−thaw cycles. A first NMR acquisition was carried out at 27 °C. Then, the tube was removed, and the temperature was set at 90 °C. The tube was then reintroduced (time t_0), and acquisitions were regularly performed. The progress of the reaction was monitored by the disappearance of the vinyl proton signals, by comparison of the vinyl protons of NAM and of GlcNAcAm with nonvinyl protons of GlcNAcAm (3H: H_1, H_3, H_4, 4.76−5.35 ppm) used as the internal reference. Similar experimental conditions were used with *t*BDB instead of biotin-CTA (BCBDBA). Polymer samples were precipitated in a large volume of diethyl ether, recovered by centrifugation, and finally dried under vacuum before SEC analysis.

Deprotection of the Glycopolymer Samples. Typically, for polymer sample biotin-P(NAM-*co*-ManAm), (47 mg, 4.7×10^{-6} mol) was dissolved in a CH_2Cl_2/methanol (1/2 v/v) anhydrous mixture (1.5 mL). A catalytic amount of sodium methylate (sodium methoxide, 25% (w/w) solution in methanol, 0.04 equiv) was added. The mixture was left under stirring at room temperature for 24 h. After evaporation, water was added, and the samples were mixed with some Amberlite IR120PLUS resin (Aldrich), filtrated, neutralized with sodium hydrogenocarbonate ($NaHCO_3$) solution, and purified by dialysis using Slide-A-Lyzer Dialysis Cassettes (Pierce) with a 3,500 molecular weight cutoff (MWCO) for samples with expected molecular weights lower

Scheme 1. Synthetic Route to the Preparation of P(NAM-*co*-GlcNAcAm) and P(NAM-*co*-ManAm) Glycopolymers, and Biotin-PNAM Homopolymer

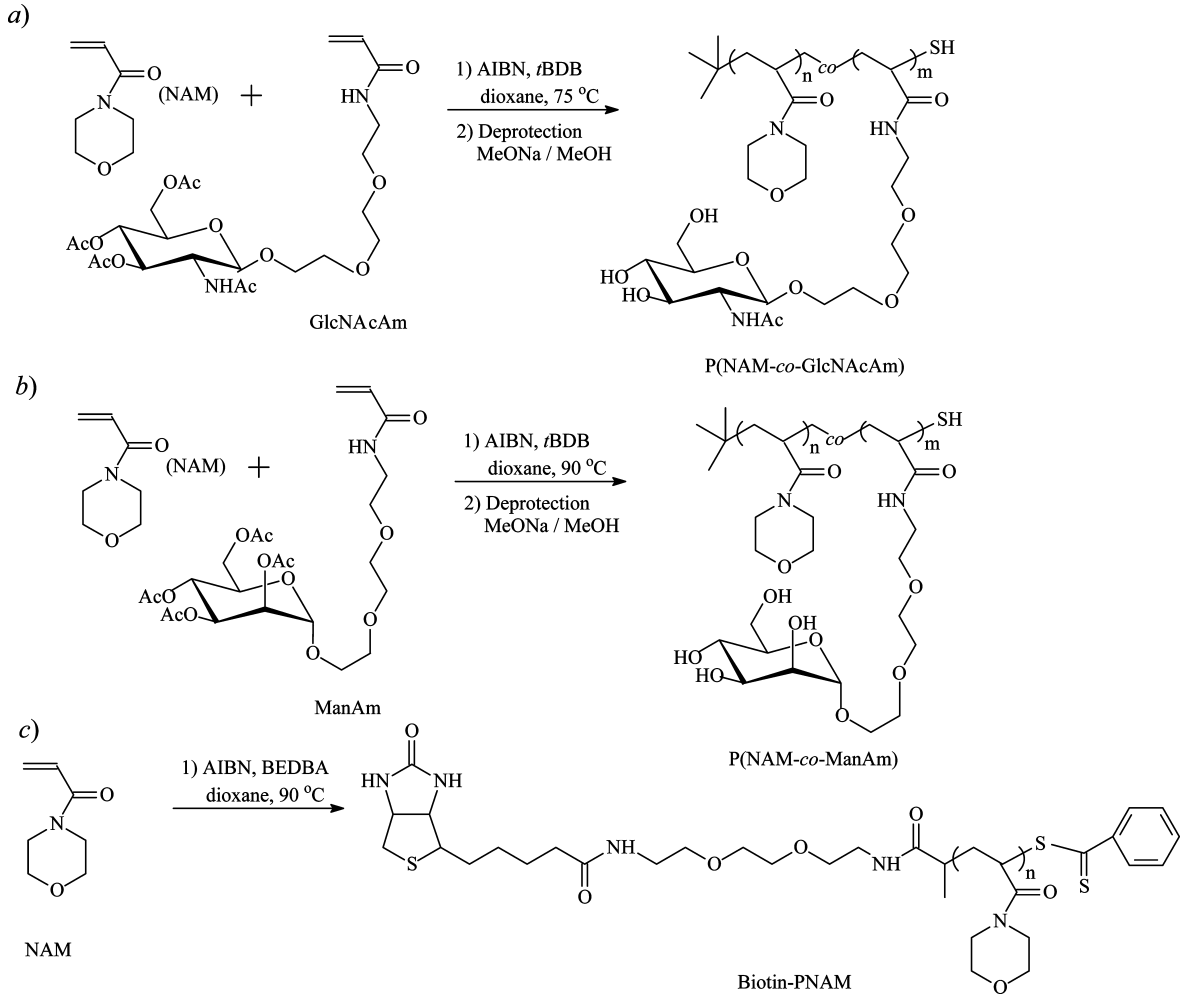

than 10,000 g·mol^{-1} and a 10,000 MWCO for all other polymers as shown in Table 1.

Formation of Gold Glyconanoparticles (AuNPs). The following protocol is carried out for the synthesis of gold glyconanoparticles, and detailed results are shown in Table 2. Polyethylene glycol having terminal thiol groups (PEG-SH) and the (non) biotinylated glycopolymer were mixed together in an aqueous solution containing $HAuCl_4$ and Irgacure-2959 at a fixed molar ratio of $HAuCl_4 \cdot 3H_2O$, Irgacure-2959, PEG-SH, and glycopolymer of 1:3:0.8:0.2, respectively. This mixture was stirred at room temperature for 10 min. The clear solution was then irradiated for 5 min in a Rayonet photoreactor (Southern N.E. Ultraviolet Co.) using 16 75W UV lamps having a 350 nm wavelength. The color of the final solution changes to purple or pink, indicating the formation of gold nanoparticles. These gold nanoparticle solutions showed very good colloidal stability over several weeks.

Characterization. *NMR.* ^{1}H NMR spectra were recorded on a 200 MHz Bruker AC 200 spectrometer or on a 500 MHz Varian Unity Plus 500 spectrometer, at 25 °C in *d*-chloroform ($CDCl_3$).

Glycopolymer SEC Analysis. Molecular weight distributions of the protected glycopolymers were determined by SEC in THF (SDS, 99%), using a Waters column (Styragel HR4E). The flow rate was maintained at 1 mL·min^{-1} using a Waters 1515 isocratic HPLC pump. Analyses were performed by injection of 20 μL of polymer solution (10 mg·mL^{-1}) in THF. Detection was performed using a Waters 2410 differential refractometer. The molecular weight and polydispersity data were determined using the Waters Breeze software package, according to a PNAM calibration.

Nanoparticle Size Analysis. A model 802 Viscotek DLS instrument operating at a laser wavelength of 825−832 nm was used for particle size measurements in highly dilute aqueous gold dispersions. TEM analyses were also performed to determine the sizes of gold nanoparticles on a Hitachi 800 transmission electron microscope at an acceleration voltage of 200 kV. The samples for TEM were prepared by placing a drop of the nanoparticle solution on carbon coated copper grids.

Diffractive Optics Technology (DOT) Measurements. DotLab data were measured on a Diffractive Optics Technology (DOT) system from Axela Biosensors Inc.; the sensor chip was composed of polystyrene as the substrate and avidin groups have been attached on the surface. PBS buffer was used as the eluent. The nanoparticle samples were loaded into the sensor according to the designed program, the binding events were taking place on the surface of the sensor chip by avidin−biotin interactions, and the height of the diffractive pattern was increased (Scheme 3). The increase in signals was detected synchronously using a laser-based optical system, and the real-time data generated are presented in dotLab software.

RESULTS AND DISCUSSION

Syntheses of Homopolymer and Statistical Copolymers Using RAFT Polymerization. *N*-Acryloylmorpholine (NAM), an acrylamide derivative, has received enormous attention for

Scheme 2. Synthetic Route to the Preparation of Biotinylated Thiol-Terminated Glycopolymers, Biotin-P(NAM-*co*-GlcNAcAm) and Biotin-P(NAM-*co*-ManAm)

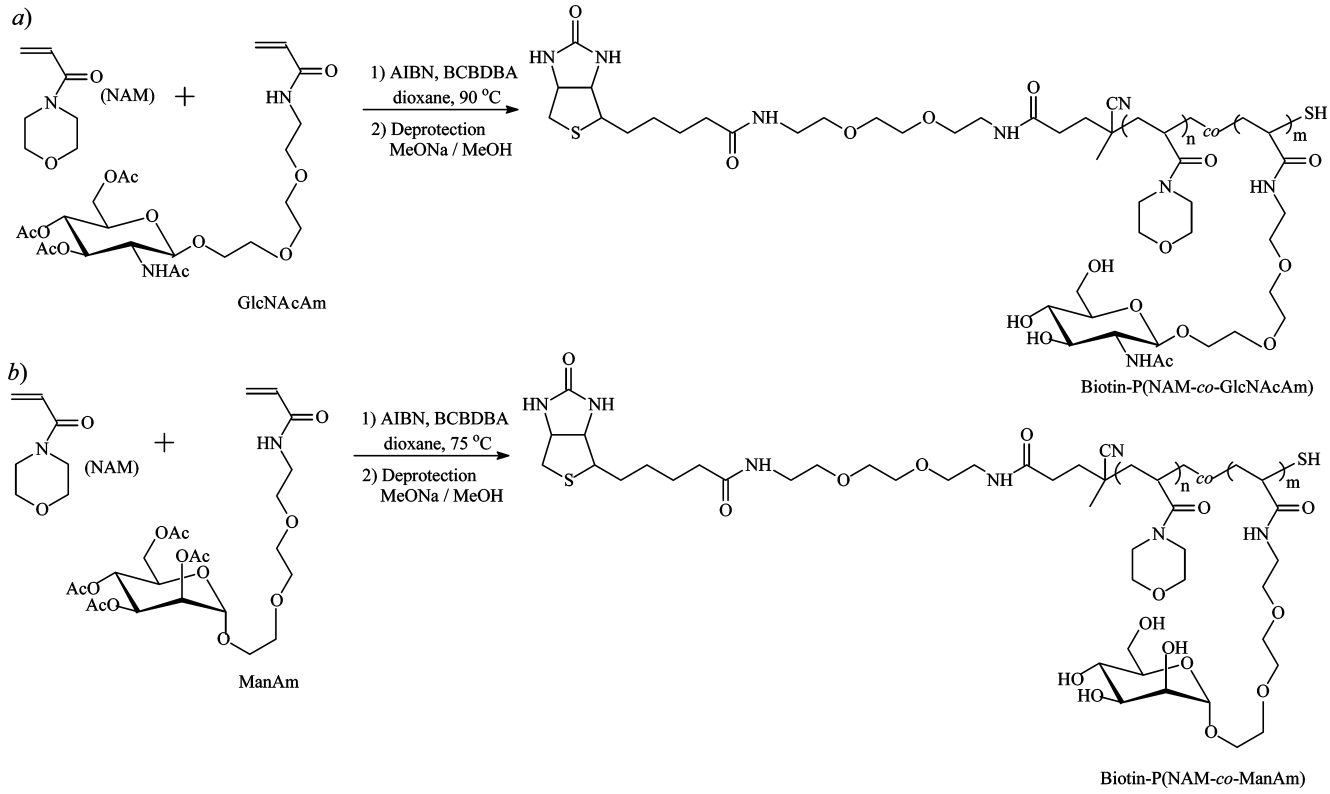

Table 1. Summary of Molecular Parameters of Synthesized Biotinylated and Nonbiotinylated Polymers

sample name	global conv. (%)	$M_{n\ calc.}$ (g·mol^{-1})	$M_{n\ calc.}$ (g·mol^{-1})	$M_{n\ exp.}$ (g·mol^{-1})	M_w/M_n (PDI)	NAM (DP)	sugar (DP)	dead chains[g]	biotin labeled[g]
biotin-PNAM$_{21}$	69	3,400[a]	/	3,500[d]	1.08[d]	21	0	9%	91%
biotin-PNAM$_{287}$	74	37,700[a]	/	41,200[e]	1.06[e]	287	0	9%	91%
P(NAM$_{234}$-*co*-GlcNAcAm$_{52}$)	93	61,200[b]	54,600[c]	62,300[f]	1.46[f]	234	52	12%	/
P(NAM$_{40}$-*co*-ManAm$_4$)	83	8,000[b]	7,300[c]	9,700[f]	1.14[f]	40	4	8%	/
biotin-P(NAM$_{225}$-*co*-GlcNAcAm$_{51}$)	85	59,300[b]	52,900[c]	53,700[f]	1.60[f]	225	51	7%	93%
biotin-P(NAM$_{40}$-*co*-ManAm$_7$)	73	10,100[b]	8,900[c]	12,700[f]	1.20[f]	40	7	6%	94%

[a] Calculated M_n (PNAM): $M_n = ([NAM]_0 \times M_{NAM} \times C_{NAM}/[CTA]_0) + M_{CTA}$. [b] Calculated M_n (protected form of the sugar): $M_n = (([NAM]_0 \times M_{NAM} \times C_{NAM} + [sugar]_0 \times M_{sugar\ protected} \times C_{sugar})/[CTA]_0) + M_{CTA}$. [c] Calculated M_n (deprotected form of the sugar): $M_n = (([NAM]_0 \times M_{NAM} \times C_{NAM} + [sugar]_0 \times M_{sugar\ deprotected} \times C_{sugar})/[CTA]_0) + M_{CTA}$. [d] Experimental M_n and PDI, determined by MALDI-TOF MS. [e] Experimental M_n and PDI, determined by SEC/RI/LS in aqueous phase (borate buffer). [f] Experimental M_n (protected form of the sugar) and PDI, determined by SEC/THF with a PNAM calibration. [g] Calculated value.

Table 2. DLS Results for the Synthesized Biotinylated and Nonbiotinylated Gold Nanoparticles via a Photochemical Process, Where the Molar Ratios of $HAuCl_4 \cdot 3H_2O$, Irgacure-2959, PEG-SH, and Synthetic Polymers Were Fixed at 1:3:0.8:0.2, Respectively

ref (AuNPs)	AuNPs prepared from relative polymers	DLS mass distribution		
		$\langle R_h \rangle$/nm	% area	% RSD
611ab	biotin-PNAM$_{21}$	6.2	99.4	8.8
612ab	biotin-PNAM$_{287}$	5.1	100	16.6
613ab	P(NAM$_{234}$-*co*-GlcNAcAm$_{52}$)	5.6	100	13.0
614ab	P(NAM$_{40}$-*co*-ManAm$_4$)	4.0	100	43.0
615ab	biotin-P(NAM$_{225}$-*co*-GlcNAcAm$_{51}$)	6.7	99.3	17.3
616ab	biotin-P(NAM$_{40}$-*co*-ManAm$_7$)	5.2	100	25.4

its special outstanding features such as the good solubility of PNAM in a wide range of solvents and its virtual lack of toxicity. The synthesized polymers were also used for various biological applications (*37–39*).

With the development of living radical polymerization, reversible addition−fragmentation chain transfer (RAFT) polymerization has proved to be a robust technique for the polymerization of the NAM monomer (*21, 33–35*). Among the studied dithiobenzoates reported by Favier et al. (*21*), *tert*-butyl dithiobenzoate (*t*BDB) has been shown to be a very efficient RAFT agent for NAM polymerization. Well-defined PNAM homopolymers with controlled dimension could be obtained in the presence of *t*BDB using AIBN as the initiator in 1,4-dioxane.

In order to study the specific carbohydrate−lectin interactions, two monomers containing carbohydrate moieties, a mannose derivative, the 8-acrylamido-3,6-dioxaoctyl 2,3,4,6-tetra-*O*-acetyl-α-D-mannopyranoside (ManAm), and a *N*-Acetyl-glucosamine derivative, the 8-acrylamido-3,6-dioxaoctyl 2-acetamido-3,4,6-tri-*O*-acetyl-2-deoxy-β-D-glucopyranoside (GlcNAcAm), were synthesized and copolymerized with NAM to get the targeted P(NAM-*co*-ManAm) and P(NAM-*co*-GlcNAcAm) copolymers. The conversions of monomers were high (above 80%), and well-controlled polymer chains were obtained as shown in Scheme 1 and Table 1. Their polymerization degrees were calculated to be P(NAM$_{40}$-*co*-ManAm$_4$) and P(NAM$_{234}$-*co*-GlcNAcAm$_{52}$) from the ^{1}H NMR and SEC results.

The RAFT technique is a versatile polymerization process that can be applied to the polymerization of many different monomers both in aqueous and organic solvents. Moreover, it is rather easy to introduce a ligand at the α-chain-end using an appropriate functional RAFT agent. A small biomolecule, biotin, was chosen to be introduced at the terminus of the RAFT agent.

Scheme 3. Schematic Illustration of Surface Bimolecular Recognitions of Biotinylated Surface-Functionalized Gold Glyco-Nanoparticles Interacting with Avidin and Lectin in Sequence on the dotLab Sensor Surface

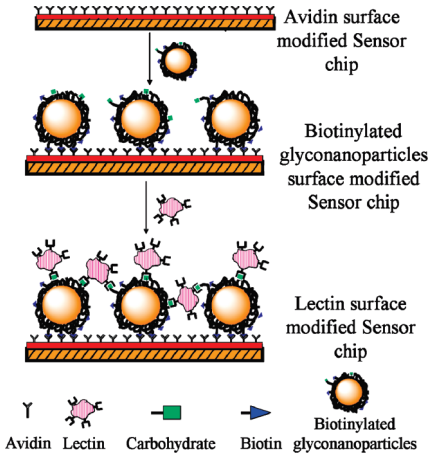

Using this kind of method, the terminal α-end of each polymer chain contains, in theory, one biotin group. On the basis of this principle, two biotin CTAs, *N*-[8-((+)-biotinamido)-3,6-dioxaoctyl]-2-[[2-phenyl-1-thioxoethyl] thiopropanamide (BEDBA) and *N*-[8-((+)-biotinamido)-3,6-dioxaoctyl]-2-[[2-phenyl-1-thioxo]thio]-4-cyano-pentanoate (BCBDBA), possessing stable bonds between the biotin and the dithioester moieties (amide and ether bonds) were synthesized to perform the homopolymerization of the NAM monomer and statistical copolymerization of NAM with ManAm or GlcNAcAm, respectively.

The synthesis of BEDBA has already been reported in the literature (*33*). BCBDBA, a new biotinylated RAFT agent, was synthesized using an approach similar to that for BEDBA (detailed synthesis and characterization are shown in Supporting Information). After activation of the carboxyl groups using *N*-hydroxysuccinimide (NHS) to form a succinimide-terminated RAFT agent, the biotin moiety (EZ-Link Biotin PEO-Amine) was introduced. These biotin-CTAs proved to be very efficient for the synthesis of the homopolymers of NAM and for the copolymerization of NAM with a protected galactose derivative (*33, 35*). The biotin-PNAM, biotin-P(NAM-*co*-ManAm), and biotin-P(NAM-*co*-GlcNAcAm) copolymers bearing the biotin moiety were synthesized as shown in Scheme 2, and detailed information is collected and presented in Table 1 and Figure 1. After polymerization for 30 min to 2 h, the targeted statistical glycopolymers in protected form were obtained. The global monomer conversion is about 85% and 73% for biotin-P(NAM-*co*-GlcNAcAm) and biotin-P(NAM-*co*-ManAm) copolymers, respectively. From the conversion values, the calculation of the DP was determined and gave biotin-P(NAM_{40}-*co*-$ManAm_7$) and biotin-P(NAM_{225}-*co*-$GlcNAcAm_{51}$). SEC traces show a monomodal peak with a low polydispersity index for biotin-P(NAM_{40}-*co*-$ManAm_7$) and a monomodal peak with a little broad polydispersity index for biotin-P(NAM_{225}-*co*-$GlcNAcAm_{51}$) as shown in Figure 1c. The experimental M_n and M_w/M_n values of biotin-P(NAM_{40}-*co*-$ManAm_7$) and biotin-P(NAM_{225}-*co*-$GlcNAcAm_{51}$) were determined as 12,700 g·mol^{-1} and 1.20 and 53,700 g·mol^{-1} and 1.60, respectively, which is consistent with the theoretical molecular weight calculated from the conversion values using ^{1}H NMR monitoring of the copolymerization. The end-label biotin functionalization was also calculated to be above 90%, which means that almost each polymer chain has a biotin group at the α terminus.

Using *t*BDB and biotin-CTAs as the RAFT agents, six different kinds of polymer chains were obtained via the RAFT process, and then six telechelic water-soluble glycopolymers (bearing a thiol group at the chain-end), named as biotin-$PNAM_{21}$, biotin-$PNAM_{287}$, P(NAM_{234}-*co*-$GlcNAcAm_{52}$), P(NAM_{40}-*co*-$ManAm_4$), biotin-P(NAM_{225}-*co*-$GlcNAcAm_{51}$), and biotin-P(NAM_{40}-*co*-$ManAm_7$), were generated after deprotection of the sugar rings by the addition of sodium methylate in methanol. The ^{1}H NMR spectra before and after deprotection are shown in Figure S2 in Supporting Information. It should be noted that two special samples, the biotin-P(NAM_{225}-*co*-$GlcNAcAm_{51}$) and biotin-P(NAM_{40}-*co*-$ManAm_7$), are our focused products because they possess both biotin groups and carbohydrate moieties and could be used to investigate biomolecular recognition, especially for the specific (or nonspecific) binding of different lectins. The other samples are used as control samples to evaluate nonspecific binding.

Fabrication of Gold Glyconanoparticles via a Photochemical Process. Gold nanoparticles have received enormous attention because of their unique optical and electronic properties (*1*). To improve their biocompatibility and colloidal stability, the gold nanoparticles were usually surface modified by thiol terminated water-soluble polymers such as PEG chains. Recently, biocompatible gold glyconanoparticles have become the focus of intense interest in biology because surface-functionalized nanoparticles containing bioactive groups such as biotin and carbohydrates could be used as model systems to investigate the biological recognition phenomena involving carbohydrates and proteins.

Gold nanoparticles were usually synthesized by two well-known methods, the Burst and Turkevish methods. Recently, a novel photochemical method reported by Scaiano et al. (*7*) has been used to prepare gold nanoparticles using UV-irradiation. This new method has attracted much attention as the sizes and shapes of gold nanoparticles could be justly controlled by the intensity of UV radiation. They have reported the preparation of highly disperse and stable gold nanoparticles via a photochemical reduction of $HAuCl_4$ with a water-soluble photoinitiator, Irgacure-2959, which decomposes quantitatively in the presence of UV light at a wavelength of 350 nm. Protein-stabilized gold nanoparticles and biotinylated glyconanoparticles have also been reported by our group using this photochemical method (*8, 9*). This new method has proved to be an easy strategy in generating surface-functionalized gold nanoparticles using RAFT-synthesized polymers. However, in the case of those glyconanoparticles, the carbohydrate moieties were introduced to bring hydrophilicity and biocompatibility but were not appropriate to recognize lectins since the sugar ring (galactose) was linked by the C-6 position. Hence, another synthetic strategy was chosen here for the carbohydrate derivatives so that the resulting glycopolymers were bearing the carbohydrate in the C-1 position, then were presenting a structure especially favorable for specific lectin recognition.

In order to study the biomolecular recognition of different proteins and carbohydrates, the functionalized monodisperse gold colloids bearing carbohydrate and biotin moieties on the surface were prepared using photochemical reduction. A mixture of Irgacure-2959, $HAuCl_4$, copolymer, and PEG-SH, at a molar ratio of 3:1:0.2:0.8, was first dissolved in filtered distilled deionized water. The resulting pale yellow solution was then placed in a photochemical reactor for a period of approximately 5−10 min. The clear solution changes from pale yellow to pink, indicating the formation of gold nanoparticles. For purification, the gold colloid solution was then dialyzed against water. It should be noted that the *in situ* reduction minimizes the formation of disulfide bridges between the thiol-terminated polymers.

Particle size measurements of the formed gold nanoparticles were obtained by dynamic light scattering (DLS), and the data were collected after purification. The results are tabulated in

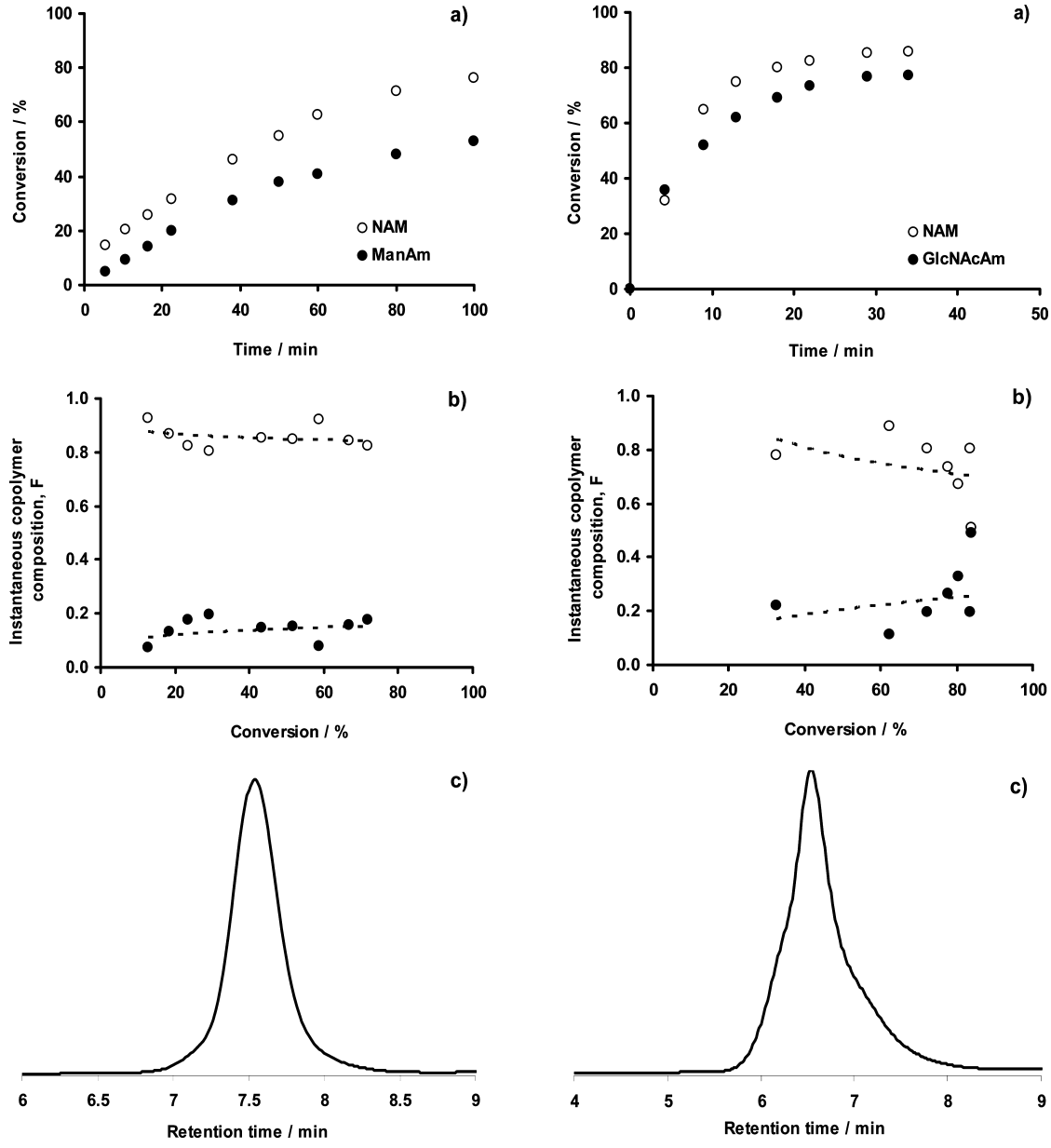

Figure 1. Monomer conversions (a), copolymer compositions (b), and SEC analysis (c) for NAM/ManAm copolymerization (left) and for NAM/GlcNAcAm copolymerization (right) using BCBDBA as the RAFT agent.

Table 2. The sizes of nanoparticles were about 4−6 nm in radius, and the polydispersities were below 0.2. This clearly shows that the mixture of the glycopolymer and -PEG-SH resulted in the formation of relatively monodisperse gold nanoparticles. The obtained gold nanoparticles were very stable, and the sizes of the glyconanoparticles did not change over weeks, which is indicative of the very high stability similar to that of PEGylated gold colloids (*12*). To further characterize the nanoparticles, the P(NAM_{234}-*co*-$GlcNAcAm_{52}$)-functionalized nanoparticles (613ab) were chosen to measure their sizes and shapes using transmission electron microscopy (TEM). Figure 2 shows the spherical and uniform morphology of these gold glyconanoparticles with a size of 4−6 nm in diameter. It should be noted that the smaller size from the TEM image may reveal only the visible gold core compared with that from DLS results. Concerning the stability, the interaction gold-thiol group is generally considered as a strong interaction. A constant diameter (and diameter distribution) was observed over weeks, which indicates a good stability of the gold nanoparticles produced. Glycopolymers, PNAM and PEG, are all biocompatible polymers used in the surface functionalization of the nanoparticles.

Diffraction Optics Technology (DOT). With the development of optical biosensors, a novel diffractive optics technology (DOT) has emerged for the potential applications in the immunoassays fields (*40*). It takes advantage of the inherent properties of diffractive optics to offer label-free real-time measurements and delivers a cost-effective, robust, optical biosensor that detects biomolecular binding even at low concentrations.

The dotLab system used includes precision fluidic control of reagents, buffers, and samples, a proprietary integrated optical assembly designed to function with the dotLab sensor, and software for acquisition, control, and user-interface. The used plastic consumable sensors consist of the polystyrene substrates and avidin-modified surfaces, and the modified surfaces possess nonrandom patterns, which were exposed to coherent light, and then well-defined diffractive images were produced. As the samples bearing biotin groups are loaded in the sensor, the

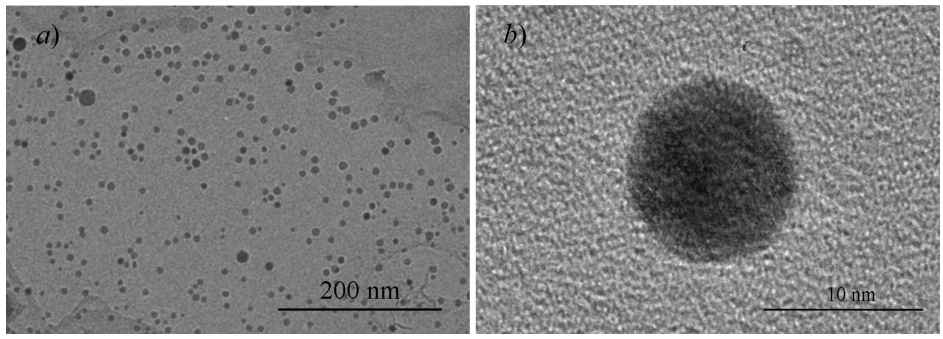

Figure 2. Typical TEM images of glyconanoparticles (613ab) prepared from the P(NAM_{234}-*co*-$GlcNAcAm_{52}$) glycopolymer.

samples are immobilized onto the surface of the sensor via the well-known biotin−avidin interactions that lead to an increase in the height of the diffractive pattern. This in turn increases the diffractive efficiency and diffractive order intensity monitored by a photodiode, and an increased signal of diffractive intensity is shown simultaneously by the software. Owing to the special design of the dotLab sensor with an integrated prism situated below the flow channel, we could monitored biomolecular binding in real time and in complex media because the light source interrogates the diffractive grating without passing through the bulk solution.

Biomolecular Recognition Involving the Carbohydrates and Lectins Detected via DOT. The surface-functionalized gold glyconanoparticles, prepared via the photochemical method, were used to study the availability of the carbohydrates and biotin toward biomolecular recognition processes. Several reference samples were used. The biotinylated nanoparticles (611ab and 612ab) without carbohydrate moieties were prepared from biotin-$PNAM_{21}$ and biotin-$PNAM_{287}$, respectively. The glyconanoparticles (613ab and 614ab) without biotin groups were prepared from P(NAM_{234}-*co*-$GlcNAcAm_{52}$) and P(NAM_{40}-*co*-$ManAm_4$), respectively. It should be noted that the biotinylated glyconanoparticles (615ab and 616ab) elaborated from biotin-P(NAM_{225}-*co*-$GlcNAcAm_{51}$) and biotin-P(NAM_{40}-*co*-$ManAm_7$) possess both biotin and carbohydrate moieties. However, the carbohydrate moieties are different (α-D-mannoside and *N*-acetyl *β*-D-glucosaminoside) and can be used as models to study the biomolecular specific recognition involving carbohydrates and lectin proteins.

Lectins are carbohydrate-binding proteins which possess a high degree of specificity toward carbohydrates. They play an important role in biological recognition phenomena involving cells and proteins, and some lectins have been widely used as a model system to understand the molecular basis of how the proteins recognize carbohydrates. It has been shown that some lectins were found on the surface of mammalian liver cells which specifically recognize galactose residues. The recognition of lectins and carbohydrates essentially occurs via multiple weak interactions (*25*). In order to further study the specific binding of carbohydrates and lectins, the lectins Concanavalin A (Con A) and wheat germ agglutinin (WGA), were chosen since they are known to specifically interact with α-D-mannoside and *N*-acetyl *β*-D-glucosaminoside moieties, respectively, that are the carbohydrates present on the prepared gold glyconanoparticles to study biomolecular recognition via dotLab measurements.

We first investigated the availability of the biotins incorporated on the surface of the nanoparticles to specifically interact with avidin located on the surface of the sensor using four control samples. The glyconanoparticles (613ab and 614ab) prepared from P(NAM_{234}-*co*-$GlcNAcAm_{52}$) and P(NAM_{40}-*co*-$ManAm_4$) (negative control samples), and two biotinylated nanoparticles (611ab and 612ab) prepared from biotin-$PNAM_{21}$ and Biotin-$PNAM_{287}$ (positive control samples), respectively, were loaded in the dotLab biosensor, and the results are shown in Figure 3. Because of the absence of biotin groups on the surface, the gold nanoparticles (613ab and 614ab) could not be immobilized on the avidin coated sensor chip. The recovery of the initial signal after wash is indicative of the fact that the gold nanoparticles were not attached on the surface of the sensor chip. However, after the biotinylated nanoparticles (611ab and 612ab) were injected into the dotLab instrument containing a preloaded avidin coated sensor chip, a signal could be observed and remained even after the wash with buffer (see Figure 3a and b), which is indicative of the specific interaction of the biotinylated nanoparticles with the avidin-coated sensor chip. These results are consistent with the work of Borisenko and co-workers regarding the aggregation of biotinylated mouse monoclonal antiNT-proBNP onto the streptavidin coated dotLab sensor (*40*) and our groups' recently reported work (*41*).

When the biotinylated glyconanoparticles (615ab and 616ab) elaborated from biotin-P(NAM_{225}-*co*-$GlcNAcAm_{51}$) and biotin-P(NAM_{40}-*co*-$ManAm_7$) were loaded into the dotLab sensor, higher responses were observed as shown in Figures 4 and 5. Because of the presence of biotin on the surface of glyconanoparticles, the nanoparticles remained immobilized on the surface of the avidin-sensor chip even after the wash with buffer.

Two different lectin solutions, Con A and WGA, were loaded following the immobilization of the biotinylated glyconanoparticles on the sensor chip. For *N*-acetyl glucosamine based carbohydrates, after the WGA lectin loading, a high response was observed while, when the same lectin solution was introduced onto PNAM-coated nanoparticles (611ab and 612ab), no increase of signal was observed because of the lack of carbohydrate groups on the surface of the nanoparticles. This indicates that there is no influence of PNAM itself on the carbohydrate/lectin interactions. The fact that the response was still present after the wash clearly showed the specific biomolecular interaction of *N*-Acetyl *β*-D-glucosaminoside residues of (615ab) with WGA. On the contrary, in the cross-experiment, almost no response was observed after the injection of Con A solution, which indicated a low nonspecific interaction and was consistent with the QCM and SPR results reported by Zhang et al. (*28*).

In addition, a strong signal was obtained after the injection of Con A solution to the immobilized glyconanoparticles (616ab) on the sensor chip, showing the specific and expected interactions of Con A with α-D-mannoside, and almost no response was observed when WGA was injected. In both cases, the cross-experiment indicated a low (<10%) nonspecific interaction between lectins and carbohydrates. This clearly demonstrates that the specific interaction of different carbohydrates and lectins such as α-D-mannoside (**Man**) with Con A and *N*-acetyl *β*-D-glucosaminoside (**GlcNAc**) with WGA could be investigated using this biosensing instrument. It further confirmed that the gold nanoparticles are carriers, and the outer carbohydrate moieties seem like many antennae increasing the specific

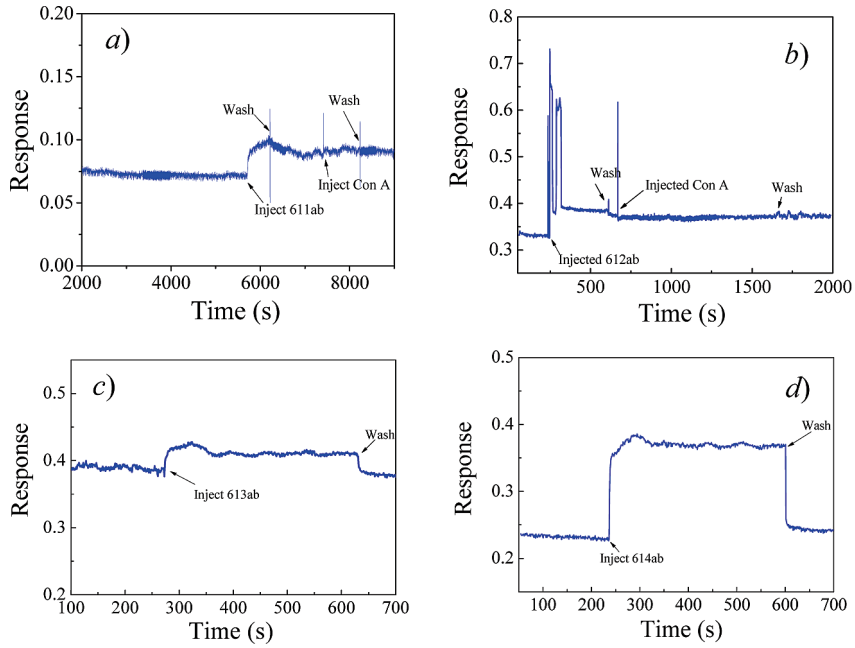

Figure 3. DotLab responses of gold nanoparticles prepared from biotin-PNAM$_{21}$ (611ab), biotin-PNAM$_{287}$ (612ab), P(NAM$_{234}$-*co*-GlcNAcAm$_{52}$) (613ab), and P(NAM$_{40}$-*co*-ManAm$_4$) (614ab) polymers.

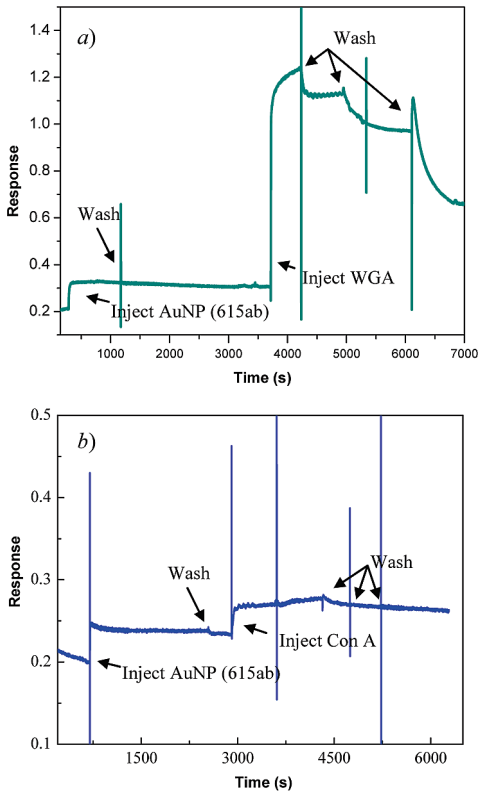

Figure 4. DotLab responses of biotinylated gold glyconanoparticles (615ab) prepared from the biotin-P(NAM$_{225}$-*co*-GlcNAcAm$_{51}$) glycopolymer with WGA (a) and Con A (b) lectins.

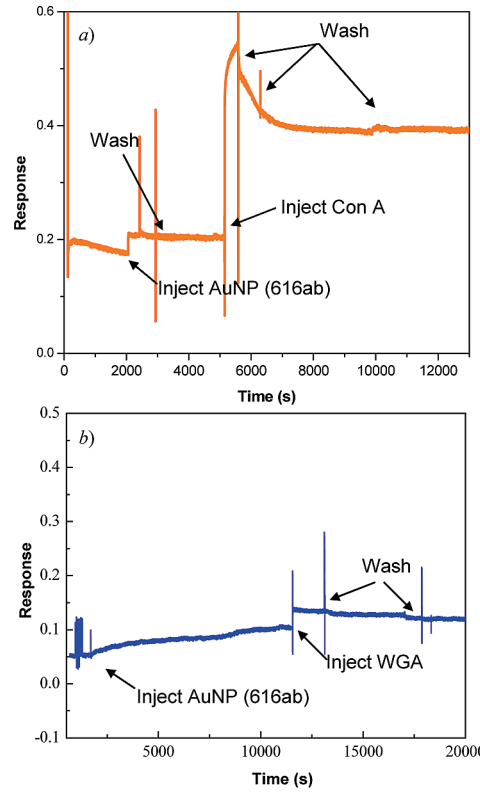

Figure 5. DotLab responses of biotinylated gold glyconanoparticles (616ab) prepared from the biotin-P(NAM$_{40}$-*co*-ManAm$_7$) glycopolymer with Con A (a) and WGA (b) lectins.

interaction of lectins and carbohydrates for the cluster glycoside effect. It should be noted that the number of carbohydrate moieties present on the surface of the nanoparticle and how many of those interact with the lectin are important parameters for this study. While this could potentially be calculated, we did not have all the parameters to exactly determine the number of chains per particle and hence the number of carbohydrate groups per particle. For this study, we just wanted to explore the specific recognition of given carbohydrate groups toward specific lectin. Besides, as the carbohydrate−lectin interactions are generally weak, it would be difficult for us to accurately measure the number of carbohydrates that are involved in those interactions.

Conclusions. Carbohydrate-based copolymers containing *N*-acetyl β-D-glucosaminopyranoside (**GlcNAc**) or α-D-mannopyranoside (**Man**) residues were prepared via RAFT polym-

erization using a biotin-CTA or *tert*-butyl dithiobenzoate as the RAFT agents. The obtained copolymers were then conjugated to the surface of gold nanoparticles by thiol chemistry that led to the formation of biotinylated or nonbiotinylated gold glyconanoparticles via a facile photochemical process. The prepared nanoparticles have uniform sizes and narrow polydispersities and are stable in water for weeks. Furthermore, the biotinylated glyconanoparticles were immobilized on the avidin-coated dotLab sensor chip because of the strong affinity between biotin and avidin, and subsequently used as the model to study the specific biomolecular recognition between lectins and carbohydrates. The specific recognitions for different carbohydrates and lectins such as α-D-mannoside with Con A and *N*-acetyl β-D-glucosaminoside with WGA were confirmed by the dotLab biosensing device. Because of the presence of PEG, biotin, and carbohydrate-based copolymer chains on the surface, these gold glyconanoparticles could be applied in biology as highly stable and biocompatible materials.

ACKNOWLEDGMENT

This work is supported jointly by Natural Sciences and Engineering Research Council of Canada and Ontario Centres of Excellence, Emerging Materials and Knowledge (OCE-EMK). We thank Axela Biosensors Inc. (Dr. Jean F. Houle) for providing the DOTLab instrument and sensor chips for this study. We thank Dr Maël Bathfield for the biotin-PNAM samples as well as Professor Stéphane Parola and Dr. Fernand Chassagneux (LMI, University of Lyon) for the TEM micrographs. We thank BioMerieux S.A. company for a Ph.D. grant for Guillaume Gody.

Supporting Information Available: Detailed synthesis and characterization of the biotinylated chain transfer agent and ^{1}H NMR data of the copolymer P(NAM-*co*-ManAm) before and after deprotection. This material is available free of charge via the Internet at http://pubs.acs.org.

LITERATURE CITED

(1) Daniel, M.-C., and Astruc, D. (2004) Gold nanoparticles: assembly, supramolecular chemistry, quantum-size-related properties, and applications toward biology, catalysis, and nanotechnology. *Chem. Rev. 104*, 293–346.

(2) Rosi, N. L., and Mirkin, C. A. (2005) Nanostructures in biodiagnostics. *Chem. Rev. 105*, 1547–1562.

(3) Brust, M., Walker, M., Bethell, D., Schiffrin, D. J., and Whyman, R. (1994) Synthesis of thiol-derivatised gold nanoparticles in a two-phase liquid-liquid system. *J. Chem. Soc. Chem. commun.* 801–802.

(4) Templeton, A. C., Wuelfing, W. P., and Murray, R. W. (2000) Monolayer-protected cluster molecules. *Acc. Chem. Res. 33*, 27–36.

(5) Grabar, K. C., Freeman, R. G., Hommer, M. B., and Natan, M. J. (1995) Preparation and characterization of Au colloid monolayers. *Anal. Chem. 67*, 735–743.

(6) Frens, G. (1973) Controlled nucleation for the regulation of the particle size in monodisperse gold solution. *Nature Phys. Sci. 241*, 20–22.

(7) McGilvray, K. L., Decan, M. R., Wang, D., and Scaiano, J. C. (2006) Facile photochemical synthesis of unprotected aqueous gold nanoparticles. *J. Am. Chem. Soc. 128*, 15980–15981.

(8) Narain, R., Housni, A., Gody, G., Boullanger, P., Charreyre, M.-T., and Delair, T. (2007) Preparation of biotinylated glyconanoparticles via a photochemical process and study of their bioconjugation to streptavidin. *Langmuir 23*, 12835–12841.

(9) Housni, A., Ahmed, M., Liu, S., and Narain, R. (2008) Monodisperse protein stabilized gold nanoparticles via a simple photochemical process. *J. Phys. Chem. C 112*, 12282–12290.

(10) Ryan, J. A., Overton, K. W., Speight, M. E., Oldenburg, C. N., Loo, L., Robarge, W., Franzen, S., and Feldheim, D. L. (2007) Cellular uptake of gold nanoparticles passivated with BSA-SV40 large T antigen conjugates. *Anal. Chem. 79*, 9150–9159.

(11) Shang, L., Wang, Y., Jiang, J., and Dong, S. (2007) pH-dependent protein conformational changes in albumin: gold nanoparticle bioconjugates: a spectroscopic study. *Langmuir 23*, 2714–2721.

(12) Liu, Y., Shipton, M. K., Ryan, J., Kaufman, E. D., Franzen, S., and Feldheim, D. L. (2007) Synthesis, stability, and cellular internalization of gold nanoparticles containing mixed peptide-poly(ethylene glycol) monolayers. *Anal. Chem. 79*, 2221–2229.

(13) Alivisatos, A. P., Johnsson, K. P., Peng, X., Wislon, T. E., Loweth, C. J., Bruchez, M. P., Jr., and Schultz, P. G. (1996) Organization of 'nanocrystal molecules' using DNA. *Nature 382*, 609–611.

(14) Mirkin, C. A., Letsinger, R. L., Mucic, R. C., and Storhoff, J. J. (1996) A DNA-based method for rationally assembling nanoparticles into macroscopic materials. *Nature 382*, 607–609.

(15) Schofield, C. L., Haines, A. H., Field, R. A., and Russell, D. A. (2006) Silver and gold glyconanoparticles for colorimetric bioassays. *Langmuir 22*, 6707–6711.

(16) Chiefari, J., Chong, Y. K., Ercole, F., Krstina, J., Jeffery, J., Le, T. P. T., Mayadunne, R. T. A., Meijs, G. F., Moad, C. L., Moad, G., Rizzardo, E., and Thang, S. H. (1998) Living free-radical polymerization by reversible addition fragmentation chain transfer: the RAFT process. *Macromolecules 31*, 5559–5562.

(17) Lowe, A. B., Sumerlin, B. S., Donovan, M. S., and McCormick, C. L. (2002) Facile preparation of transition metal nanoparticles stabilized by well-defined (co)polymers synthesized via aqueous reversible addition-fragmentation chain transfer polymerization. *J. Am. Chem. Soc. 124*, 11562–11563.

(18) Shan, J., and Tenhu, H. (2007) Recent advances in polymer protected gold nanoparticles: synthesis, properties and applications. *Chem. Commun.* 4580–4598.

(19) Corbierre, M. K., Cameron, N. S., Sutton, M., Mochrie, S. G. J., Lurio, L. B., Ruhm, A., and Lennox, R. B. (2001) Polymer-stabilized gold nanoparticles and their incorporation into polymer matrices. *J. Am. Chem. Soc. 123*, 10411–10412.

(20) Yurekli, K., Karim, A., Amis, E. J., and Krishnamoorti, R. (2003) Influence of layered silicates on the phase-separated morphology of PS-PVME blends. *Macromolecules 36*, 7256–7267.

(21) Favier, A., Charreyre, M.-T., Chaumont, P., and Pichot, C. (2002) Study of the RAFT polymerization of a water-soluble bisubstituted acrylamide derivative. 1. Influence of the dithioester structure. *Macromolecules 35*, 8271–8280.

(22) Goldstein, I. J., Iyer, R. N., Smith, E. E., and So, L. L. (1967) Protein- carbohydrate interaction. XX. The interaction of concanavalin A with sophorose and some of its derivatives. *Biochemistry 6*, 2373–2377.

(23) Hong, C.-H. (2003) *Carbohydrate-Based Drug Discovery*, Wiley-VCH, Weinheim, Germany.

(24) Lee, Y. C., and Lee, R. T. (1995) Carbohydrate-protein interactions: basis of glycobiology. *Acc. Chem. Res. 28*, 321–327.

(25) Lundquist, J. J., and Toone, E. J. (2002) The cluster glycoside effect. *Chem. Rev. 102*, 555–578.

(26) Otsuka, H., Akiyama, Y., Nagasaki, Y., and Kataoka, K. (2001) Quantitative and reversible lectin-induced association of gold nanoparticles modified with α-lactosyl-ω-mercapto-poly(ethylene glycol). *J. Am. Chem. Soc. 123*, 8226–8230.

(27) Touhami, A., Hoffmann, B., Vasella, A., Denis, F. A., and Dufrene, Y. F. (2003) Probing specific lectin-carbohydrate interactions using atomic force microscopy imaging and force measurements. *Langmuir 19*, 1745–1751.

(28) Zhang, Y., Luo, S., Tang, Y., Yu, L., Hou, K.-Y., Cheng, J.-P., Zeng, X., and Wang, P. G. (2006) Carbohydrate-protein interactions by "clicked" carbohydrate self-assembled monolayers. *Anal. Chem. 78*, 2001–2008.

(29) Hone, D. C., Haines, A. H., and Russell, D. A. (2003) Rapid, quantitative colorimetric detection of a lectin using mannose-stabilized gold nanoparticles. *Langmuir 19*, 7141–7144.

(30) La Belle, J. T., Gerlach, J. Q., Svarovesky, S., and Joshi, L. (2007) Label-free impedimetric detection of glycan-lectin interactions. *Anal. Chem. 79*, 6959–6964.

(31) Dai, Z., Kawde, A.-N., Xiang, Y., La Belle, J. T., Gerlach, J., Bhavanandan, V. P., Joshi, L., and Wang, J. (2006) Nanoparticle-based sensing of glycan-lectin interactions. *J. Am. Chem. Soc. 128*, 10018–10019.

(32) Gestwicki, J. E., Cairo, C. W., Strong, L. E., Oetjen, K. A., and Kiessling, L. L. (2002) Influencing receptor-ligand binding mechanisms with multivalent ligand architecture. *J. Am. Chem. Soc. 124*, 14922–14933.

(33) Bathfield, M., D'Agosto, F., Spitz, R., Charreyre, M.-T., and Delair, T. (2006) Versatile precursors of functional RAFT agents. Application to the synthesis of bio-related end-functionalized polymers. *J. Am. Chem. Soc. 128*, 2546–2547.

(34) Gody, G. (2008) Synthesis of saccharide monomers for preparation of gradient, alpha-functionalized and block glycopolymers by the RAFT process. Application in immobilization of biomolecules by specific recognition or covalent link, Ph.D. Thesis, University Claude Bernard, Lyon, France.

(35) Gody, G., Boullanger, P., Ladavière, C., Charreyre, M.-T., and Delair, T. (2008) Biotin α-end-functionalized gradient glycopolymers synthesized by RAFT copolymerization. *Macromol. Rapid Commun. 29*, 511–519.

(36) D'Agosto, F., Charreyre, M. T., Veron, L., Llauro, M. F., and Pichot, C. (2001) Kinetic study of free-radical solution copolymerization of *N*-acryloylmorpholine with an activated ester-type monomer, *N*-acryloxysuccinimide. *Macromol. Chem. Phys. 202*, 1689–1699.

(37) Torchilin, V. P., Trubetskoy, V. S., Whiteman, K. R., Caliceti, P., Ferruti, P., and Veronese, F. M. (1995) New synthetic amphiphilic polymers for steric protection of liposomes in vivo. *J. Pharm. Sci. 84*, 1049–1053.

(38) Ranucci, E., Spagnoli, G., Sartore, L., Ferruti, P., Caliceti, P., Schiavon, O., and Veronese, F. M. (1994) Synthesis and molecular weight characterization of low molecular weight end-functionalized poly(4-acryloylmorpholine). *Macromol. Chem. Phys. 195*, 3469–3479.

(39) Ushakova, V., Panarin, E., Ranucci, E., Bignotti, F., and Ferruti, P. (1995) Synthesis of low molecular weight poly(*N*-acryloylmorpholine) end-functionalized with primary amino groups, and its use as macromonomer for the preparation of poly(amidoamines). *Macromol. Chem. Phys. 196*, 2927−2939.

(40) Borisenko, V., Hu, W., Tam, P., Chen, I., Houle, J.-F., and Ausserer, W. (2006) Diffractive optics technology: a novel detection technology for immunoassays. *Clin. Chem. 52*, 2168–2170.

(41) Deng, Z. C., Li, S. Q., Jiang, X. Z., and Narain, R. (2009) Well-defined galactose- containing multi-functional copolymers and glyco-nanoparticles for biomolecular recognition processes. *Macromolecules 42*, 6393–6405.

BC900431P